

Determine the chirality of Weyl fermions from the circular dichroism spectra of time-dependent ARPES

Rui Yu^{1,*}, Hongming Weng^{2,3}, Zhong Fang^{2,3}, Hong Ding^{2,3}, and Xi Dai^{2,3,†}

¹*Department of Physics, Harbin Institute of Technology, Harbin 150001, China*

²*Beijing National Laboratory for Condensed Matter Physics,
and Institute of Physics, Chinese Academy of Sciences, Beijing 100190, China and*

³*Collaborative Innovation Center of Quantum Matter, Beijing 100190, China*

(Dated: December 15, 2015)

Abstract

We show that the intensity of pumped states near Weyl point is different when pumped with left- and right-handed circular polarized light, which leads to a special circular dichroism (CD) in time-dependent angle resolved photoemission spectra (ARPES). We derive the expression for the CD of time-dependent ARPES, which is directly related to the chirality of Weyl fermions. Based on the above derivation, we further propose a method to determine the chirality for a given Weyl point from the CD of time-dependent ARPES. The corresponding CD spectra for TaAs has then been calculated from the first principle, which can be compared with the future experiments.

PACS numbers: 79.60.-i, 71.55.Ak, 73.20.At

* yurui@hit.edu.cn

† daix@iphy.ac.cn

I. INTRODUCTION

The research on topological quantum states has emerged as one of the major topics in condensed matter physics in recent years. It was ignited by the discovery of two-dimensional (2D) and three-dimensional (3D) topological insulators (TIs) [1, 2] and received significant attention again by the discovery of 3D topological semimetals. In 3D topological semimetals the conduction and valence bands touch at certain points in the Brillouin zone and generate nontrivial band topology [3]. Up to now, there are three types of topological semimetals: Weyl semimetals, Dirac semimetals and node-line semimetals. For Weyl semimetals, the band touching points are doubly degenerate and distributed in the Brillouin zone as isolated points, which can be viewed as “magnetic monopoles” in momentum space [4]. According to the so called “no-go theorem” [5–7], Weyl points in lattice systems always appear in pairs with definite and opposite chirality. The Dirac semimetals can be generated by overlapping two Weyl fermions with opposite chirality at the same k -point, which has fourfold degenerate at the band touching points and can be only protected by additional crystalline symmetry [8, 9]. For node-line semimetals, the band touching points form closed loops in Brillouin zone around the Fermi level [10–13].

The breakthrough in topological semimetals research happened after the material realization of Dirac semimetal states in Na_3Bi and Cd_3As_2 [8, 9, 14–18]. Starting from Dirac semimetals, one can obtain Weyl semimetals by breaking either time-reversal [19–22] or inversion symmetry [23–27]. Recently, a family of nonmagnetic and noncentrosymmetric 3D Weyl semimetals, the stoichiometric TaAs, TaP, NbAs and NbP, was first predicted theoretically [28, 29] and then verified experimentally [30–37]. The intriguing expected properties characterizing the Weyl semimetal have been checked carefully in this family of materials. The surface Fermi arcs have been observed in most of these materials from ARPES experiments [30, 31, 34–37]. The nontrivial π Berry’s phase has been experimentally accessed by analyzing the Shubnikov de Haas oscillations in TaAs [33, 38]. The negative magneto-resistivity due to chiral anomaly has been observed in TaAs [33]. However all the above experiments can only prove the existence of the Weyl points but can not determine the chirality for each particular Weyl points, which is the key issue in the physics of Weyl semimetals. In this paper, we show that the chirality of a particular Weyl point can be determined from the CD spectra of the time-dependent ARPES experiments.

II. WEYL HAMILTONIAN

The most general Hamiltonian expanded near a Weyl point can be expressed by the following two-band model

$$H_W = \sum_{i,j} k_i a_{ij} \sigma_j = (k_x, k_y, k_z) \hat{a} (\sigma_x, \sigma_y, \sigma_z)^T, \quad (1)$$

where $i, j = x, y, z$ and the matrix a connects the pseudo-spin space σ and momentum space \mathbf{k} . Eq. (1) can be rewrite as

$$H_W = \chi \sum_{i,j} k_i \tilde{a}_{ij} \sigma_j, \quad (2)$$

where $\chi = \text{sign}[\text{Det}(a)]$ is the chirality of the Weyl fermions. The new matrix \tilde{a} are defined as $\tilde{a} = \chi a$ and possesses positive determinant $\text{sign}[\text{Det}(\tilde{a})] = +1$. The matrix \tilde{a} can be decomposed by single value decomposition (SVD) as $\tilde{a} = S \Lambda D$, where Λ is a diagonal matrix with three positive elements denoted as λ_1, λ_2 and λ_3 . S and D are two real orthogonal matrices and we can choose the gauge condition that both of them take positive determinant, with which the new coordinates can be uniquely defined according to the “principle axes” in the momentum and pseudo spin spaces as $(k_1, k_2, k_3) = (k_x, k_y, k_z)S$ and $(\sigma_1, \sigma_2, \sigma_3) = (\sigma_x, \sigma_y, \sigma_z)D^T$, respectively. Rotating the coordinate systems into the principle axis defined as 1, 2 and 3 in both momentum and pseudo spin spaces, Eq. (2) can be rewritten as

$$H_W = \chi \sum_{i=1,2,3} \lambda_i k_i \sigma_i. \quad (3)$$

In Weyl semimetal materials, the Weyl points always come in pairs with opposite chirality. In the following sections, we will discuss how to detect the chirality for a given Weyl point from the CD of time-dependent ARPES experiment. In the experimental setup as illustrated in Fig. 1, the circular polarized light is shined onto a Weyl semimetal in order to pump electrons from the occupied states to the unoccupied states. Since the purpose is to selectively pump the “chiral electrons” from the lower branch to the upper branch of a Weyl cone using chiral photons (see Fig. 2) [39], the energy of the pumping photons needs to be within the linear range of the Weyl dispersion, which is roughly a few tens meV for TaAs, thus a THz source is required. The continuing-pumped unoccupied states can then be probed by regular bulk-sensitive ARPES, such as soft x-ray ARPES commonly used in the study of Weyl semimetals [30, 31, 34–37].

III. CD SPECTRA OF PUMPED STATES

We start from the Hamiltonian Eq. (3) and take $\chi = +1$ as an example to discuss the CD spectra of pumped states for Weyl fermions. The eigenvalues of Eq. (3) are given as $E_{c/v} = \pm((\lambda_1 k_1)^2 + (\lambda_2 k_2)^2 + (\lambda_3 k_3)^2)^{1/2}$, and the eigenfunctions for conduction and valence bands are given as

$$|u_c\rangle = \begin{bmatrix} \cos\frac{\theta_k}{2} e^{-i\frac{\phi_k}{2}} \\ \sin\frac{\theta_k}{2} e^{+i\frac{\phi_k}{2}} \end{bmatrix} \text{ and } |u_v\rangle = \begin{bmatrix} -\sin\frac{\theta_k}{2} e^{-i\frac{\phi_k}{2}} \\ +\cos\frac{\theta_k}{2} e^{+i\frac{\phi_k}{2}} \end{bmatrix}, \quad (4)$$

where $\cos\theta_k = \frac{\lambda_3 k_3}{|E|}$ and $\tan\phi_k = \frac{\lambda_2 k_2}{\lambda_1 k_1}$.

To consider the coupling of electrons and pump light, we start from the microscopic Hamiltonian of an electron with spin-orbit coupling which is given by

$$H_0 = \frac{\mathbf{p}^2}{2m} + V + \frac{\hbar}{4m^2}(\nabla V \times \mathbf{p}) \cdot \mathbf{s}, \quad (5)$$

where \mathbf{p} is momentum operator, V is crystal potential, and \mathbf{s} is electron spin operator. The Hamiltonian for systems coupled to the electromagnetic field is obtained via the Peierls substitution $\mathbf{p} \rightarrow \mathbf{p} - e\mathbf{A}$, where \mathbf{A} is the vector potential of the electromagnetic field. The electron-photon interaction term can then be obtained as $H_{int} = H_0(\mathbf{p} - e\mathbf{A}) - H_0(\mathbf{p})$ leading to

$$H_{int} = -e\mathbf{A} \cdot \mathbf{v}, \quad (6)$$

where

$$v_i = \frac{\partial H_W}{\partial k_i} = \chi \lambda_i \sigma_i, \quad (7)$$

is the velocity operator, where $i = 1, 2, 3$.

Suppose in the ideal case the chemical potential is located right at the Weyl point, then the pumping rate from the lower branch to the upper branch caused by the light is determined by the following matrix element

$$M_{cv} = \langle u_c | \mathcal{A} \cdot \mathbf{v} | u_v \rangle, \quad (8)$$

where \mathcal{A} is the Fourier transform of vector potential \mathbf{A} . For the circular polarized light we have

$$\begin{aligned} \mathcal{A}_x &= A_0(\cos\theta_l \cos\phi_l + \eta i \sin\phi_l), \\ \mathcal{A}_y &= A_0(\cos\theta_l \sin\phi_l - \eta i \cos\phi_l), \\ \mathcal{A}_z &= -A_0 \sin\theta_l. \end{aligned} \quad (9)$$

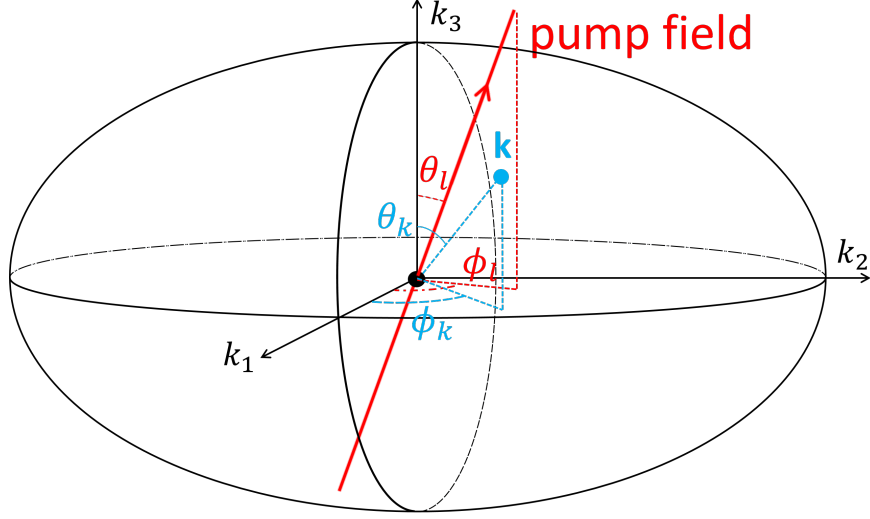


Figure 1. Diagram of the experimental geometry. Circular polarized light can be continuously rotated by θ_l and ϕ_l as shown in the figure.

where $\eta = \pm 1$ indicate the right/left-handed circular polarized light and θ_l and ϕ_l are angles describing the propagating direction of the injecting light as illustrated in Fig. 1.

First we consider the simplest case with the light injecting from one of the principal axis, say along \hat{k}_3 axis with $\theta_l = 0$ and $\phi_l = 0$. The vector potential of light in Eq. (9) is then simplified as

$$\mathcal{A} = A_0(1, -\eta i, 0), \quad (10)$$

Therefore, the matrix element in Eq. (8) takes the formula as

$$M_{cv} = \langle u_c | \frac{1}{2} (\mathcal{A}_- v_+ + \mathcal{A}_+ v_-) | u_v \rangle, \quad (11)$$

where $\mathcal{A}_\pm = \mathcal{A}_1 \pm i\mathcal{A}_2 = A_0(1 \pm \eta)$ and $v_\pm = v_1 \pm iv_2$. For the states in the $+\hat{k}_3$ axis, where $\theta_k = 0$, we get $|u_c\rangle_{+\hat{k}_3} = \begin{pmatrix} 1 \\ 0 \end{pmatrix}$ and $|u_v\rangle_{+\hat{k}_3} = \begin{pmatrix} 0 \\ 1 \end{pmatrix}$ as expressed in Eq. (4). To keep the discussions simple, we suppose that $\lambda_1 = \lambda_2$. Then it is easy to check that only the v_+ operator contribute nonzero matrix element between $|u_c\rangle_{+\hat{k}_3}$ and $|u_v\rangle_{+\hat{k}_3}$ states. Meanwhile, the requirement of \mathcal{A}_- being nonzero lead to $\eta = -1$. These results mean that for Weyl fermions with chirality $\chi = 1$, the occupied states in the $+\hat{k}_3$ axis can only be pumped by the left-handed circular polarized photons. For the states in the $-\hat{k}_3$ axis, they can only be pumped by the right-handed circular polarized photons as illustrated in Fig. 2(a). Whereas for $\chi = -1$, with the same argument as discussed above, we find that the situation is just

the opposite, where the states at the $\pm\hat{k}_3$ axis can only be pumped by the right/left-handed circular polarized light as illustrated in Fig. 2(d).

The pumping process induced by the circular polarized light will be eventually balanced by the relaxation processes in the crystal and form a steady state. The occupation intensity of the excited states in such a steady state can be obtained as [40]

$$I_\eta \propto |M_{cv}|^2 A_c(E_c) A_v(E_v) = |M_{cv}|^2 / (\pi^2 \epsilon_c \epsilon_v), \quad (12)$$

where $A_v(\omega) = \frac{1}{\pi} \frac{\epsilon_v}{[\omega - E_v]^2 + \epsilon_v^2}$ and $A_c(\omega) = \frac{1}{\pi} \frac{\epsilon_c}{[\omega - E_c]^2 + \epsilon_c^2}$ denote the spectral functions of the initial and final states in the non-interaction case. The parameters ϵ_v and ϵ_c reflect the finite lifetime of electrons. The CD spectra are defined as $I_{CD} = I_{RCP} - I_{LCP}$, which measures the difference of I with right- and left-handed circular polarized pumping light. Therefore the CD values in the $\pm\hat{k}_3$ axis can be calculated as

$$I_{CD}^{\pm\hat{k}_3} \propto \mp 4\chi A_0^2 \lambda_1^2 / (\pi^2 \epsilon_c \epsilon_v), \quad (13)$$

which shows that the CD spectra take opposite values at $\pm\hat{k}_3$ axis and its sign directly related to the chirality χ as shown in Fig. 2(b,e).

The above results indicate that we can determine the chirality for a given Weyl point by checking the CD of time-dependent ARPES. But there is one problem which needs to be clarified. In the previous paragraph, we have set the light propagating direction to be identical to the positive direction of the absolute coordinate system and obtain the above results. It seems that we need to know in advance that which direction is positive (according to the gauge fixing condition defined above) for a given principle axis, which is not possible experimentally. Actually this is not necessary due to the following reason. Let's consider another possibility that the circular polarized light is applied anti-parallel to the absolute \hat{k}_3 direction. the CD spectra can be obtained as shown in Fig. 2(c,f). Comparing the results in Fig. 2(b,c,e,f), we find that if we define the propagating direction of the circular polarized light as the reference direction, the results for both situations become identical, namely for Weyl point with chirality $\chi = 1$ the CD of the time-dependent ARPES will be positive (negative) for momentum \mathbf{k} anti-parallel (parallel) to the propagating direction of light as illustrated in Fig. 2(b,c), while for $\chi = -1$ the CD spectra will be positive (negative) for momentum \mathbf{k} parallel (anti-parallel) to the propagating direction of light as illustrated in Fig. 2(e,f). Therefore the above results can be used to determine the chirality of a Weyl point purely by experiments.

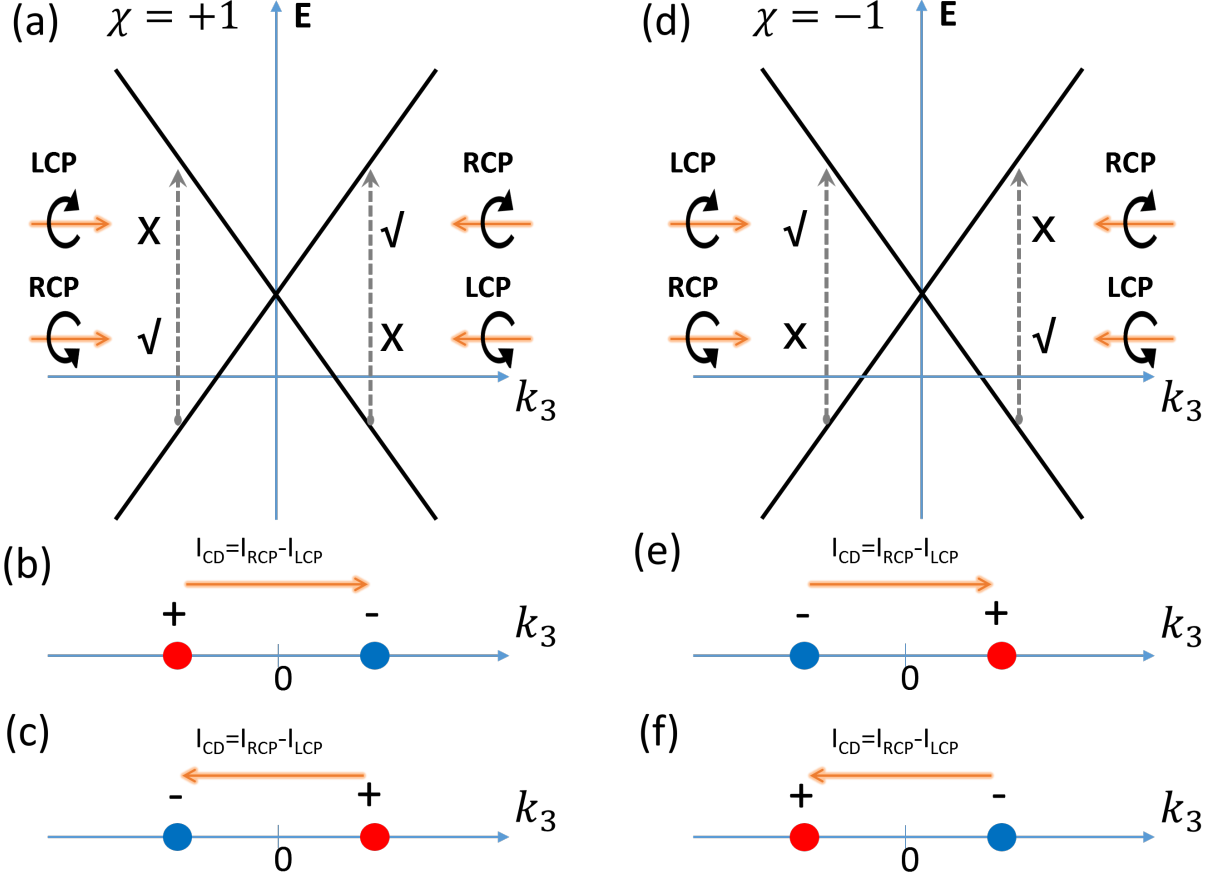


Figure 2. (a) In the condition of $\lambda_1 = \lambda_2$, for the Weyl fermions with chirality $\chi = 1$, the occupied states in the $+\hat{k}_3$ axis can only be pumped to the empty states by left (right)-handed circular polarized light injected along \hat{k}_3 ($-\hat{k}_3$) direction, while for the states in the $-\hat{k}_3$ axis, they can only be pumped by right (left)-circular polarized light injected along \hat{k}_3 ($-\hat{k}_3$) direction. (b, c) The CD values with light injected along \hat{k}_3 and $-\hat{k}_3$ direction for $\chi = 1$. The CD value is positive (negative) for \mathbf{k} anti-parallel (parallel) to the propagating direction of the light. (d, e, f) for the Weyl fermions with chirality $\chi = -1$. The CD value is positive (negative) for \mathbf{k} parallel (anti-parallel) to the propagating direction of the light.

For the more general case that the pump field injected with angles θ_l and ϕ_l , the CD spectra at \mathbf{k} point with angles θ_k and ϕ_k can be calculated as

$$I_{CD} \propto -4\chi A_0^2 (\lambda_1 \lambda_2 \cos\theta_k \cos\theta_l + \lambda_3 \sin\theta_k \sin\theta_l * (\lambda_2 \cos\phi_k \cos\phi_l + \lambda_1 \sin\phi_k \sin\phi_l)) / (\pi^2 \epsilon_c \epsilon_v). \quad (14)$$

We discuss the CD spectra for the general case in the following section.

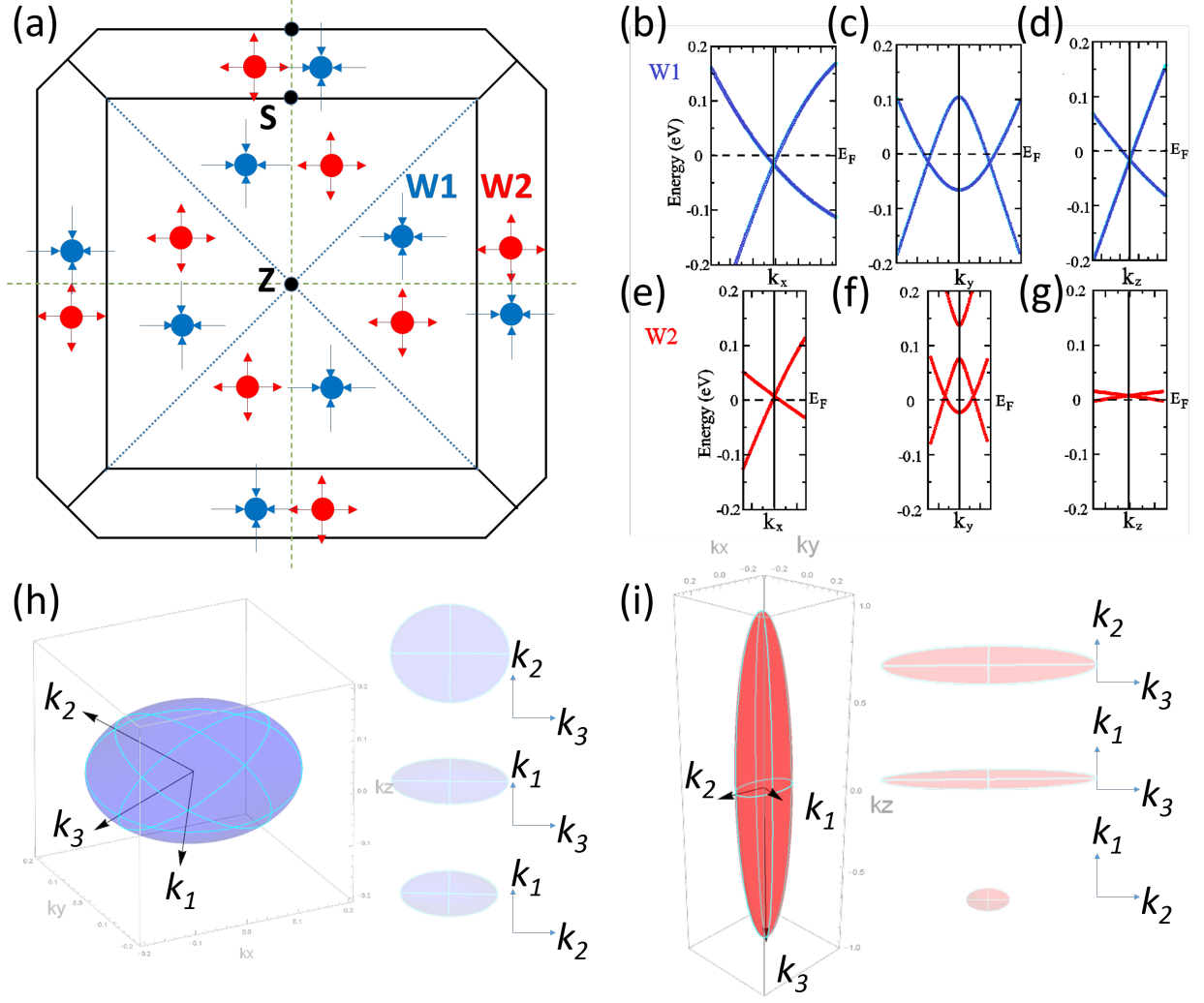


Figure 3. (a) The distribution of the 12 pairs of Weyl points in BZ for TaAs compounds. The red color for the Weyl point with chirality $\chi = 1$ and blue color for $\chi = -1$. The two nonequivalent pairs are marked as W1 and W2. The 4 pairs of W1 type Weyl points showing in (a) are on the top of another 4 W1 pairs, which are invisible. The bands dispersion near W1 point and W2 point are shown in (b-d) and (e-g) respectively. (h,i) The ellipse shape isenergic surface near W1 and W2 points and their top view along three principle axes.

IV. WEYL POINTS IN TAAS

The new discovered TaAs family materials are the first verified realistic materials that contain Weyl points near the Fermi level. Totally there are 12 pairs of Weyl points in TaAs

as shown in Fig. 3(a). The two nonequivalent pairs are marked as W1 and W2. At each Weyl point, the low-energy effective Hamiltonian takes the formula as expressed in Eq. (1). The matrix a in Eq. (1) for W1 and W2 can be obtained by fitting with the first-principle calculations and expressed as

$$a^{W1} = \begin{bmatrix} 2.657 & -2.526 & 0.926 \\ 0.393 & -2.134 & 3.980 \\ -1.200 & -3.530 & 1.193 \end{bmatrix}, \quad (15)$$

and

$$a^{W2} = \begin{bmatrix} 1.849 & 2.531 & 0.269 \\ 1.849 & 1.388 & -4.910 \\ 0.428 & -0.302 & 0.006 \end{bmatrix}. \quad (16)$$

The energy dispersion and the isenergetic surface near W1 and W2 are shown in Fig. 3(b-i). By performing the SVD, we can get the singular values of a^{W1} and a^{W2} as $\lambda_1^{W1} = 6.055$, $\lambda_2^{W1} = 2.834$, $\lambda_3^{W1} = 2.340$, $\lambda_1^{W2} = 5.564$, $\lambda_2^{W2} = 2.899$ and $\lambda_3^{W2} = 0.520$ in unit of $\text{eV} \cdot \text{Bohr}$. The principal axes of the ellipse for the isenergetic surface near W1 and W2 are obtained as $\hat{k}_1^{W1} = -(0.478, 0.694, 0.537)$, $\hat{k}_2^{W1} = (-0.811, 0.115, 0.573)$, $\hat{k}_3^{W1} = (-0.336, 0.710, -0.618)$, $\hat{k}_1^{W2} = (0.257, 0.966, 0.011)$, $\hat{k}_2^{W2} = (0.966, -0.257, -0.007)$ and $\hat{k}_3^{W2} = (-0.004, 0.012, -0.999)$ as shown in Fig. 3(h,i).

With the help of Eq. (14), The CD spectra of time-dependent ARPES for Weyl point can be obtained as

$$I_{CD} \propto -4\chi A_0^2 \lambda_1 \lambda_2 \cos\theta_k / (\pi^2 \epsilon_c \epsilon_v), \quad (17)$$

with the pump field injected along the \hat{k}_3 direction. For the pump field injected along the $-\hat{k}_3$ direction, the CD spectra are

$$I_{CD} \propto +4\chi A_0^2 \lambda_1 \lambda_2 \cos\theta_k / (\pi^2 \epsilon_c \epsilon_v). \quad (18)$$

Using the criterion discussed in previous paragraph, the positive (negative) CD values for \mathbf{k} anti-parallel (parallel) to the propagating direction of the light indicate that $\chi = +1$, whereas the positive (negative) CD values for \mathbf{k} parallel (anti-parallel) to the propagating direction of the light indicate that $\chi = -1$ as shown in Fig. 4. This criterion works even for the light propagating direction slightly deviates from the principle axis.

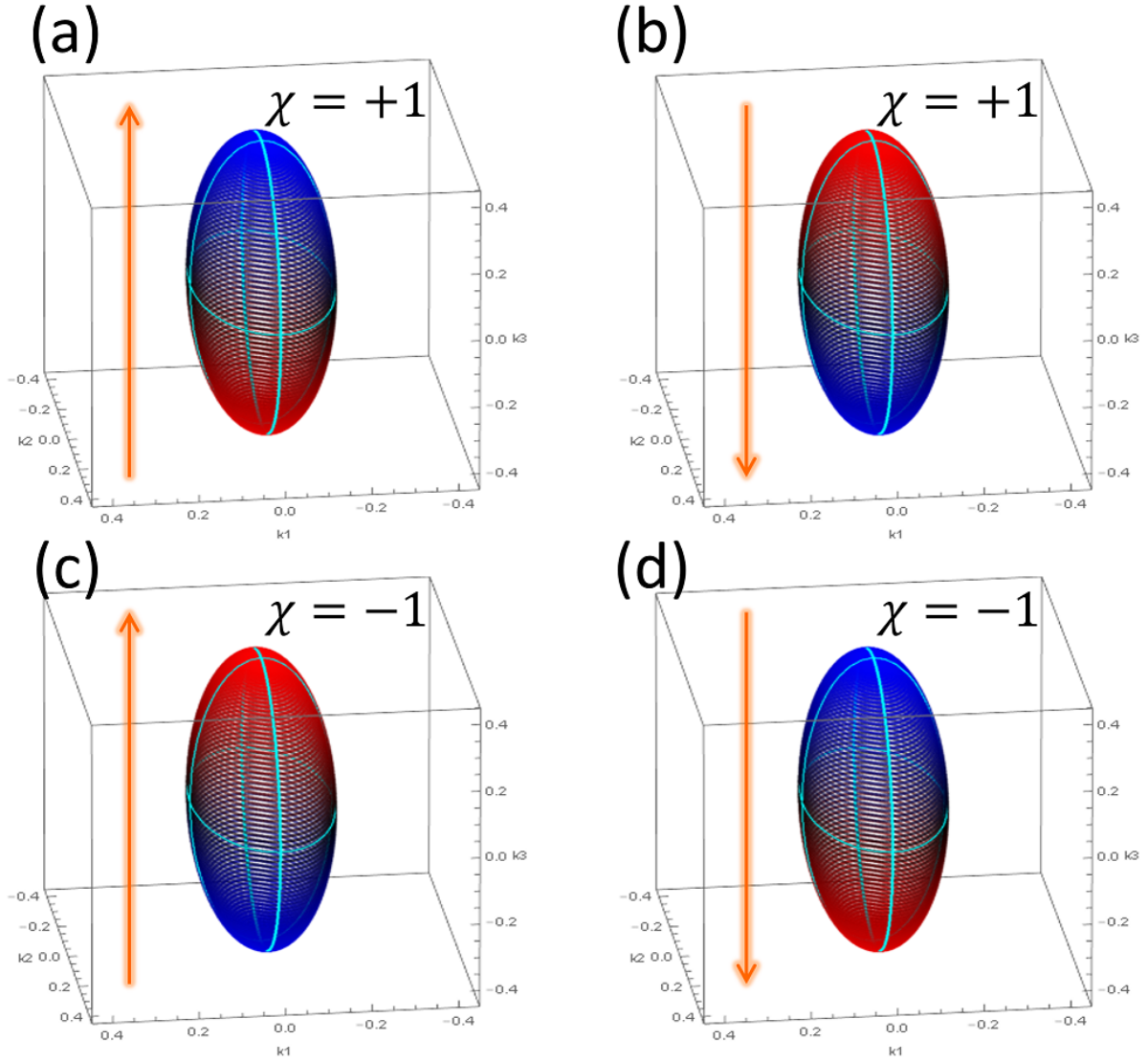


Figure 4. The CD spectra for Weyl point with chirality $\chi = 1$ pumped with field (a) parallel and (b) anti-parallel to $+\hat{k}_3$ principle axis. The red color indicate the positive CD values and blue color for the negative CD values. In this case, the positive (negative) CD values is in the anti-parallel (parallel) direction of the propagating direction of the light. (c) and (d) for Weyl point with chirality $\chi = -1$. In this case, the positive (negative) CD values is in the parallel (anti-parallel) direction of the propagating direction of the light.

V. CONCLUSION

In summary, we have investigated the CD of time-dependent ARPES near Weyl points and show that the CD values is related to the chirality of Weyl fermions, which provide a

way to determine the chirality of the given Weyl point by checking the sign of CD values along the propagating direction of the light. The corresponding CD spectra for Weyl point in TaAs compound have then been calculated, which can be compared with the future CD time-dependent ARPES experiments.

Acknowledgments: This work was supported by the National Natural Science Foundation of China, the 973 program of China (No.2013CB921700), and the “Strategic Priority Research Program (B)” of the Chinese Academy of Sciences (No.XDB07020100). R.Y. acknowledges funding from the Fundamental Research Funds for the Central Universities (Grant No.AUGA5710059415).

-
- [1] M. Z. Hasan and C. L. Kane, *Rev. Mod. Phys.* **82**, 3045 (2010).
 - [2] X.-L. Qi and S.-C. Zhang, *Rev. Mod. Phys.* **83**, 1057 (2011).
 - [3] G. E. Volovik, *The Universe in a Helium Droplet* (Oxford, 2009).
 - [4] Z. Fang, N. Nagaosa, K. S. Takahashi, A. Asamitsu, R. Mathieu, T. Ogasawara, H. Yamada, M. Kawasaki, Y. Tokura, and K. Terakura, *Science* **302**, 92 (2003).
 - [5] H. Nielsen and M. Ninomiya, *Phys. Lett. B* **105**, 219 (1981).
 - [6] H. Nielsen and M. Ninomiya, *Nucl. Phys. B* **185**, 20 (1981).
 - [7] H. Nielsen and M. Ninomiya, *Nucl. Phys. B* **193**, 173 (1981).
 - [8] Z. Wang, Y. Sun, X.-Q. Chen, C. Franchini, G. Xu, H. Weng, X. Dai, and Z. Fang, *Phys. Rev. B* **85**, 195320 (2012).
 - [9] Z. Wang, H. Weng, Q. Wu, X. Dai, and Z. Fang, *Phys. Rev. B* **88**, 125427 (2013).
 - [10] A. A. Burkov, M. D. Hook, and L. Balents, *Phys. Rev. B* **84**, 235126 (2011).
 - [11] H. Weng, Y. Liang, Q. Xu, R. Yu, Z. Fang, X. Dai, and Y. Kawazoe, *Phys. Rev. B* **92**, 045108 (2015).
 - [12] Y. Kim, B. J. Wieder, C. L. Kane, and A. M. Rappe, *Phys. Rev. Lett.* **115**, 036806 (2015).
 - [13] R. Yu, H. Weng, Z. Fang, X. Dai, and X. Hu, *Phys. Rev. Lett.* **115**, 036807 (2015).
 - [14] A. Pariari, P. Dutta, and P. Mandal, *Phys. Rev. B* **91**, 155139 (2015).
 - [15] L. P. He, X. C. Hong, J. K. Dong, J. Pan, Z. Zhang, J. Zhang, and S. Y. Li, *Phys. Rev. Lett.* **113**, 246402 (2014).
 - [16] M. Neupane, S.-Y. Xu, R. Sankar, N. Alidoust, G. Bian, C. Liu, I. Belopolski, T.-R. Chang,

- H.-T. Jeng, H. Lin, A. Bansil, F. Chou, and M. Z. Hasan, *Nat. Commun.* **5** (2014).
- [17] Z. K. Liu, B. Zhou, Y. Zhang, Z. J. Wang, H. M. Weng, D. Prabhakaran, S.-K. Mo, Z. X. Shen, Z. Fang, X. Dai, Z. Hussain, and Y. L. Chen, *Science* **343**, 864 (2014).
- [18] Z. K. Liu, J. Jiang, B. Zhou, Z. J. Wang, Y. Zhang, H. M. Weng, D. Prabhakaran, S. K. Mo, H. Peng, P. Dudin, T. Kim, M. Hoesch, Z. Fang, X. Dai, Z. X. Shen, D. L. Feng, Z. Hussain, and Y. L. Chen, *Nat. Mater.* **13**, 677 (2014).
- [19] X. Wan, A. M. Turner, A. Vishwanath, and S. Y. Savrasov, *Phys. Rev. B* **83**, 205101 (2011).
- [20] G. Xu, H. Weng, Z. Wang, X. Dai, and Z. Fang, *Phys. Rev. Lett.* **107**, 186806 (2011).
- [21] A. A. Burkov and L. Balents, *Phys. Rev. Lett.* **107**, 127205 (2011).
- [22] L. Balents, *Physics* **4**, 36 (2011).
- [23] S. Murakami, *New J. Phys.* **9**, 356 (2007).
- [24] G. B. Halász and L. Balents, *Phys. Rev. B* **85**, 035103 (2012).
- [25] L. Lu, Z. Wang, D. Ye, L. Ran, L. Fu, J. D. Joannopoulos, and M. Soljacic, *Science* **349**, 622 (2015).
- [26] J. Liu and D. Vanderbilt, *Phys. Rev. B* **90**, 155316 (2014).
- [27] M. Hirayama, R. Okugawa, S. Ishibashi, S. Murakami, and T. Miyake, *Phys. Rev. Lett.* **114**, 206401 (2015).
- [28] H. Weng, C. Fang, Z. Fang, B. A. Bernevig, and X. Dai, *Phys. Rev. X* **5**, 011029 (2015).
- [29] S.-M. Huang, S.-Y. Xu, I. Belopolski, C.-C. Lee, G. Chang, B. Wang, N. Alidoust, G. Bian, M. Neupane, C. Zhang, S. Jia, A. Bansil, H. Lin, and M. Z. Hasan, *Nat. Commun.* **6**, 7373 (2015).
- [30] B. Q. Lv, N. Xu, H. M. Weng, J. Z. Ma, P. Richard, X. C. Huang, L. X. Zhao, G. F. Chen, C. E. Matt, F. Bisti, V. N. Strocov, J. Mesot, Z. Fang, X. Dai, T. Qian, M. Shi, and H. Ding, *Nat. Phys.* **11**, 724 (2015).
- [31] B. Lv, H. Weng, B. Fu, X. Wang, H. Miao, J. Ma, P. Richard, X. Huang, L. Zhao, G. Chen, Z. Fang, X. Dai, T. Qian, and H. Ding, *Phys. Rev. X* **5**, 031013 (2015).
- [32] L. X. Yang, Z. K. Liu, Y. Sun, H. Peng, H. F. Yang, T. Zhang, B. Zhou, Y. Zhang, Y. F. Guo, M. Rahn, D. Prabhakaran, Z. Hussain, S.-K. Mo, C. Felser, B. Yan, and Y. L. Chen, *Nat. Phys.* **11**, 728 (2015).
- [33] X. Huang, L. Zhao, Y. Long, P. Wang, D. Chen, Z. Yang, H. Liang, M. Xue, H. Weng, Z. Fang, X. Dai, and G. Chen, *Phys. Rev. X* **5**, 031023 (2015).

- [34] S.-Y. Xu, N. Alidoust, I. Belopolski, Z. Yuan, G. Bian, T.-R. Chang, H. Zheng, V. N. Strocov, D. S. Sanchez, G. Chang, C. Zhang, D. Mou, Y. Wu, L. Huang, C.-C. Lee, S.-M. Huang, B. Wang, A. Bansil, H.-T. Jeng, T. Neupert, A. Kaminski, H. Lin, S. Jia, and M. Zahid Hasan, *Nat. Phys.* **11**, 748 (2015).
- [35] S.-Y. Xu, I. Belopolski, N. Alidoust, M. Neupane, G. Bian, C. Zhang, R. Sankar, G. Chang, Z. Yuan, C.-C. Lee, S.-M. Huang, H. Zheng, J. Ma, D. S. Sanchez, B. Wang, A. Bansil, F. Chou, P. P. Shibayev, H. Lin, S. Jia, and M. Z. Hasan, *Science* **349**, 613 (2015).
- [36] B. Q. Lv, S. Muff, T. Qian, Z. D. Song, S. M. Nie, N. Xu, P. Richard, C. E. Matt, N. C. Plumb, L. X. Zhao, G. F. Chen, Z. Fang, X. Dai, J. H. Dil, J. Mesot, M. Shi, H. M. Weng, and H. Ding, *Phys. Rev. Lett.* **115**, 217601 (2015).
- [37] N. Xu, H. M. Weng, B. Q. Lv, C. Matt, J. Park, F. Bisti, V. N. Strocov, D. gawryluk, E. Pomjakushina, K. Conder, N. C. Plumb, M. Radovic, G. Autès, O. V. Yazyev, Z. Fang, X. Dai, G. Aeppli, T. Qian, J. Mesot, H. Ding, and M. Shi, *arXiv:1507.03983* (2015).
- [38] C. Zhang, Z. Yuan, S. Xu, Z. Lin, B. Tong, M. Z. Hasan, J. Wang, C. Zhang, and S. Jia, *arXiv:1502.00251* (2015).
- [39] C. Ching-Kit, P. A. Lee, K. S. Burch, J. H. Han, and Y. Ran, *arXiv:1509.05400* (2015).
- [40] C. Kunz, Photoemission in Solids II, edited by L. Ley and M. Cardona, Springer-Verlag, Berlin. (1979).